CHAPTER 21

Fluorescence-Lifetime Imaging Techniques for Microscopy

Chen Y. Dong,[1] Todd French,[2] Peter T. C. So,[1] C. Buehler,[1] Keith M. Berland,[3] and Enrico Gratton[1]

[1]Laboratory for Fluorescence Dynamics
Department of Physics
University of Illinois at Urbana-Champaign
Urbana, Illinois 61801

[2]Molecular Devices Corporation
Sunnyvale, California 94089

[3]Physics Department
Emory University
Atlanta, Georgia 30322

METHODS IN CELL BIOLOGY, VOL. 72

0091-679X/03 $35.00

Three different methods of fluorescence-lifetime imaging for microscopy are presented along with some examples of their use. All three methods use the frequency-domain heterodyning technique to collect lifetime data. Because of the nature of the data collection technique, these instruments can measure the correct lifetime even when the sample undergoes strong photobleaching. Each instrument has unique capabilities that complement the others.

The first microscopic-lifetime imaging technique uses a fast charge-coupled device (CCD) camera and a gated image intensifier. The camera system collects an entire lifetime image in parallel in only a few seconds. This microscope is well suited to kinetic studies of intracellular lifetime changes. The other two techniques use scanned laser source to collect sequential lifetime information pixel by pixel. One microscope uses two-photon excitation to achieve three-dimensional, confocal-like imaging without using detection pinholes. Two-photon excitation also limits the effects of out-of-plane photodamage of the sample. The second laser-scanning microscope uses a pump-probe technique for fluorescence-lifetime imaging. By measuring the cross-correlation frequency, high-frequency harmonic imaging can be achieved without high-speed detectors. The cross-correlation volume also results in three-dimensional spatial resolution equal to a confocal microscope and time resolution limited only by the laser light source.

I. Introduction

Fluorescence is a sensitive technique useful as a vital contrast-enhancement mechanism for microscopic imaging. Labeling at high specificity, fluorescence microscopy has excellent background rejection. It provides the high contrast needed to spatially resolve microscopic structures such as cellular organelles. Although the spatial relationship of the organelles is important, the functional properties of the organelles also are vital in the understanding of cellular physiology. Local physiological parameters such as the pH or molecular concentration may be revealed by fluorescence microscopic imaging. Fluorescent probes can also act as sensitive probes to local cellular environment. For example, some probes are fluorescent only in a particular pH or polarity condition. In most applications, fluorescence intensity measurements are used to monitor various processes in cells and tissues. However, intensity imaging may not be suitable for quantitative work. The measured intensity depends not only on the fluorophore environment but also on the local probe concentration, which cannot be easily determined. Quantitative measurements using concentration-independent parameters may bypass probe concentration–related artifacts. Spectra and fluorescence lifetime of a fluorescent probe are two parameters independent of the probe concentration. Techniques that exploit either spectral- or lifetime-sensitive probes can be used as environmental probes in measuring quantitatively environmental factors that affect the excited state. Consequently, ratiometric (spectral) and fluorescence-lifetime (temporal) techniques coupled to fluorescence microscopy can provide localized quantitative information of the cellular and tissue environments.

Fluorescence techniques reveal information of the molecular state of a chromophore. Spectral and polarization changes in the emitted light reveal the excited-state properties and the orientation of the transition dipole moments. To form a more complete investigation of the nature of the excited state, time-resolved measurements are required. For example, fluorescence quenching may occur because of a ground-state reaction or an excited-state reaction. Only by measuring the probe's fluorescence lifetime can one determine the nature of molecular interaction. The excited state also can be affected by the molecular environment through processes such as solvent relaxation, energy transfer, and conformational changes. This sensitivity makes fluorescent probes excellent monitors of cellular factors such as pH, viscosity, molecular concentration, and local order.

The sensitivity of fluorescence lifetime to the microenvironment has been used to measure pH (Sanders *et al*., 1995a), metal ion concentration (Piston *et al*., 1994; Lakowicz *et al*., 1994a), fluorescence resonance energy transfer (Oida *et al*., 1993; Gadella and Jovin, 1995), cellular photostress (König *et al*., 1996), and antigen processing (French *et al*., 1997). Other quantities such as molecular oxygen concentration, environmental polarity, and local order also may be measured using lifetime imaging techniques. Lifetime can also be used as a contrast-enhancing mechanism. Different fluorophore species with different lifetimes can be imaged in one picture, and the fraction of each fluorophore can be resolved within a single image element (So *et al*., 1995; Sanders *et al*., 1995b).

Time-resolved fluorescence microscopy has advanced greatly from the first single-pixel measurements (Dix and Verkman, 1990; Keating and Wensel, 1990). These first experiments deduced important cellular information such as calcium concentration or cytoplasm matrix viscosity at selected points inside a cell. Further development in fluorescence-lifetime-resolved microscopy resulted in the extension of the single-point measurements to obtain lifetime information across the entire cell. Two different approaches have been applied. The first method uses CCD cameras equipped with gain-modulated image intensifiers to collect data simultaneously across the entire image. The other approach modifies traditional confocal laser scanning microscopes and obtains time-resolved information on a point-by-point basis.

The laser scanning microscope uses a single-point detector to acquire images one point at a time. Serial acquisition systems consist of a single-point detector and a scanning mechanism to move the sample or the excitation light. Fluorescence-lifetime imaging can be achieved by adapting normal lifetime-resolved detectors and electronics to the new optical setup. Laser scanning microscopy has been used to measure three-dimensionally resolved lifetime images with confocal detection (Buurman *et al*., 1992; Morgan *et al*., 1992), two-photon excitation (Piston *et al*., 1992; So *et al*., 1995) and time-dependent optical mixing (Dong *et al*., 1995; Müller *et al*., 1995). In addition, near-field scanning optical microscopy has been used to image surface fluorescent lifetimes (Ambrose *et al*., 1994; Xie and Dunn, 1994).

Time-resolved imaging of the full field simultaneously is harder to implement. Full-field imaging generally employs a two-dimensional array detector (such as a CCD) to capture all points in an image in parallel (rather than one at a time). The problem associated with this approach is in achieving nanosecond time resolution (required for fluorescence) across a large spatial area. The basic approaches are to use a gated image intensifier coupled to a camera or a position-sensitive photomultiplier. Both frequency-domain (Wang *et al.*, 1989; Marriott *et al.*, 1991; Lakowicz and Berndt, 1991; So *et al.*, 1994; Morgan *et al.*, 1995) and time-domain (Wang *et al.*, 1991; Oida *et al.*, 1993; McLoskey *et al.*, 1996) techniques have been developed.

In this chapter, we describe the development and applications of fluorescence-lifetime imaging microscopy. Three different fluorescent-lifetime imaging microscopes that use the frequency-domain heterodyning technique are described: a CCD-based system, a two-photon laser scanning system, and a laser scanning, pump-probe (stimulated emission) technique.

II. Time-Resolved Fluorescence Methods

A. Time-Domain and Frequency-Domain Measurements

Time-resolved fluorescence measurements can be performed in two functionally equivalent ways: the time-domain or the frequency-domain approach (for further discussion, see Chapter 9). In the time domain, the impulse response of a system is probed. A fluorescent sample is illuminated with a narrow pulse of light, and the resulting fluorescence emission decay is captured with a fast recorder. A common method for reconstructing the decay profile is time-correlated single-photon counting. With this method, the time delay between the emitted photon and the excitation pulse is recorded. For a low enough emission rate (fewer than 10^5 photons per second), every photon's delay can be recorded. An entire decay curve can be reconstructed by plotting the number of photons as a function of the delay times. To properly reconstruct the decay curve, the excitation profile must also be measured so that it may be used to deconvolve the finite width of the excitation pulse from the emission profile.

The frequency-domain method measures the harmonic response of the system. The sample is excited by a sinusoidally modulated source. An arbitrarily complex modulation waveform can be decomposed into sinusoidal components such that only sinusoidal modulation needs to be discussed. The emission signal appears as a sine wave that is demodulated and phase shifted from the source (Fig. 1). The phase shift and modulation are used to obtain the lifetime of the fluorophore. For a single exponential decay, the phase (ϕ) and modulation (M) are related to the excited state lifetime (τ) by Eqs. (1) and (2), in which ω is the angular modulation frequency, or 2π times the modulation frequency. For maximum sensitivity, the angular modulation frequency should be roughly the inverse of the lifetime. Because typical lifetimes are 1–10 ns, the corresponding modulation frequencies are 20–200 MHz.

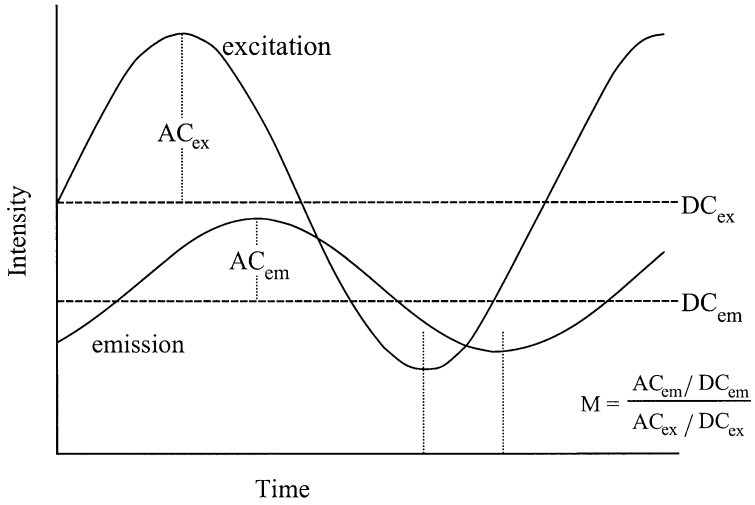

Fig. 1 Definitions of phase (ϕ) and modulation (M) in frequency domain measurements.

$$\omega\tau = \tan(\phi) \tag{1}$$

$$\omega\tau = \sqrt{\frac{1}{M^2} - 1}. \tag{2}$$

Because the emission signal is too fast to be sampled continuously, the high-frequency signal is often converted to a lower frequency. In this process of heterodyning, the frequency conversion is accomplished using a gain-modulated detector. The detector is modulated at a frequency close to the frequency of the excitation source. The result is a beating of the emission and detector modulation signals that yields a cross-correlation frequency signal that is at the difference of the frequencies.

If the source and detector frequencies are the same, the frequency-mixing process is called homodyning. Homodyning, by definition, results in a DC signal whose amplitude is proportional to the sine of the difference of the phase between the detector and the emission. To acquire the entire phase and modulation information of the emission signal, it is necessary to systematically step the phase difference between the source and detector modulation signals. Homodyning is commonly used with a fixed phase difference to collect phase-resolved data. By properly choosing the phase of the detector, one can suppress or enhance certain lifetimes. A disadvantage of homodyning is that it is more sensitive than heterodyning to spurious DC components such as stray light. Heterodyning recovers all of the high-frequency phase and modulation information in each cross-correlation period (typically 10–100 ms) and can be used for acquiring phase-resolved data as well.

For the three different time-resolved techniques, the concept of heterodyned data acquisition is used. First, we apply a synchronous averaging filter. Several cross-correlation waveforms are collected and combined to form an average waveform. This filter removes random noise by rejecting signals that are not at the cross-correlation frequency or its harmonics. The reduction of the bandwidth along with the averaging causes the signal-to-noise ratio to increase linearly with the number of waveforms averaged (Feddersen *et al.*, 1989). The next step in data reduction involved fast Fourier transform (FFT). The cross-correlation signal is uniformly sampled in time such that FFT can be used to calculate the phase and modulation. The manner in which we apply FFT is equivalent to (but simpler than) a least-squares fit of multiple sine waves to the data. Additional averaging of the sequential phase and modulation images is sometimes used in the scanning microscopes to further reduce the noise. This is a less-efficient filter, and the noise is reduced as expected from Poisson statistics.

The sampling frequency is generally chosen such that four samples are collected in one cross-correlation period (Fig. 2). To measure a signal at a given frequency,

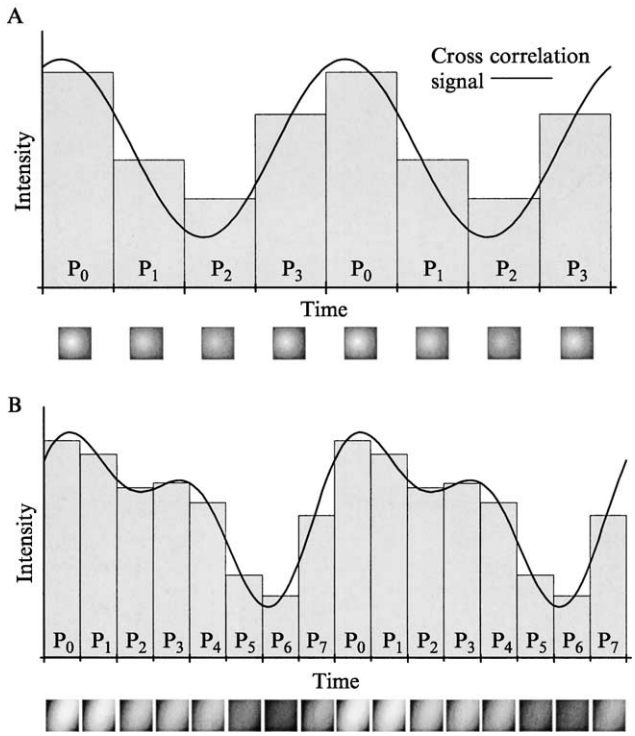

Fig. 2 Sampling of the cross-correlation signal. (A) Four images collected per cross-correlation period. (B) Eight images can reduce the error in the measurement (harmonic distortion).

the signal must be sampled at least at twice that frequency (Nyquist theorem). If noise appears as a high-frequency signal, it is better to sample at a higher rate to produce a more accurate measurement. More points sampled results in better discrimination of the various harmonics. Thus, by increasing the number of samples per cross-correlation period, higher-frequency signals (generally noise) can be more easily separated from the fundamental.

B. Simultaneous Multiple-Lifetime-Component Measurement

To discriminate more harmonics and achieve better noise rejection, more points can be sampled per period. For the first-generation microscope instruments presented in this chapter, we chose to use four points per cross-correlation period because it was faster and the higher harmonics were small compared to the fundamental frequency. However, there are situations that can benefit from measuring higher harmonics.

One such case is the simultaneous measurement of two probes with dissimilar lifetimes. To measure the two lifetimes, the phase and modulation would have to be collected in separate measurements at each of the frequencies appropriate for the given fluorophore. However, it is possible to map the two modulation frequencies to two different cross-correlation frequencies and collect the phase and modulation in one measurement. If the two cross-correlation frequencies are related by an integer multiple, they can be separated by FFT.

Consider the case of a sample consisting of two probes whose lifetimes are 1 and 1000 ns. Two appropriate modulation frequencies are 100 MHz and 100 kHz, respectively. If the laser is modulated at a mixture of 100 MHz and 100 kHz and the detector is modulated at a mixture of 100 MHz + 10 Hz and 100 kHz + 20 Hz, the two signals can be separated. The result of the heterodyning is two signals at 10 and 20 Hz that correspond to the fluorescence decay at 100 MHz and 100 kHz, respectively.

To achieve the mixing of the 100-MHz and 100-kHz signals and still produce a strong fluorescence signal, the two signals should both be sine waves. When combined with a high-frequency mixer, the result is the high-frequency signal enclosed in an envelope of the intermediate frequency signal (Fig. 3A). On heterodyning, the resultant low-frequency signal will be composed mainly of the two cross-correlation frequencies (Fig. 3B).

After measuring the phase and modulation at each frequency, it is still necessary to separate the lifetime components. The most common approach is to fit a decay scheme to the acquired data. For the example outlined in this section, it is possible to use algebraic methods to separate the two components. The algebraic method is possible whenever the two lifetimes are known to be different by several orders of magnitude.

To describe the example system, the following conventions are used. The shorter lifetime component (1 ns) will be referred to with the subscript 1. The longer component (1000 ns) will have the subscript 2. The fractional intensity

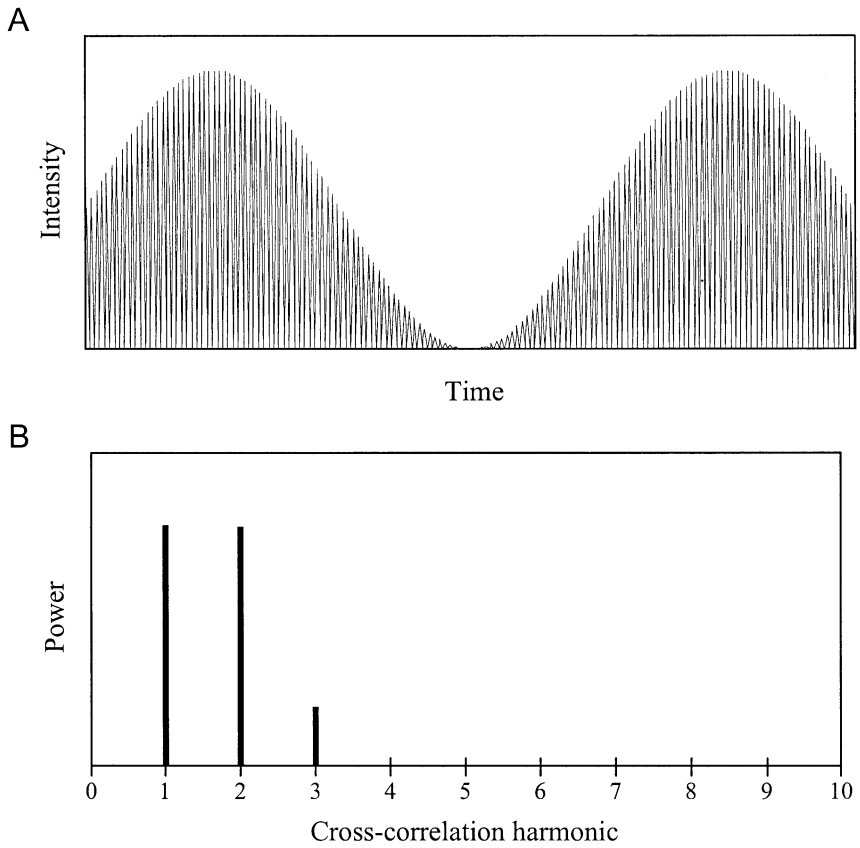

Fig. 3 Dual modulation signal. (A) The source or detector signal. (B) The low-frequency power spectrum of the heterodyned signal.

of the fluorescence contributed by the short lifetime probe is indicated by f. $(1-f)$ will be contributed by the other component.

In the frequency domain, lifetime components add as vectors. The vector sum of the phase and modulation times the fractional intensity of each component results in the measured phase and modulation of a multiple-component system. The Cartesian components of the resultant lifetime vector for a two-component system are given in Eqs. (3) and (4):

$$M_r(\omega)\cos[\phi_r(\omega)] = fM_1(\omega)\cos[\phi_1(\omega)]+(1-f)M_2(\omega)\cos[\phi_2(\omega)], \quad (3)$$

$$M_r(\omega)\sin[\phi_r(\omega)] = fM_1(\omega)\sin[\phi_1(\omega)]+(1-f)M_2(\omega)\sin[\phi_2(\omega)]. \quad (4)$$

By measuring the phase and modulation at the two frequencies appropriate for the two components ($\omega_1 \approx 1/\tau_1$, $\omega_2 \approx 1/\tau_2$), Eqs. (3) and (4) can be rearranged and

combined with Eqs. (1) and (2) to solve for each of the lifetime values and the fractional intensity:

$$f = \frac{M_r(\omega_1)}{\cos\left[\phi_r(\omega_1)\right]}, \tag{5}$$

$$\tau_1 = \frac{\tan\left[\phi_r(\omega_1)\right]}{\omega_1}, \tag{6}$$

$$\tau_2 = \frac{M_r(\omega_2)\sin\left[\phi_r(\omega_2)\right]}{\omega_2\left[M_r(\omega_2)\cos\left[\phi_r(\omega_2)\right] - f\right]}. \tag{7}$$

Table I lists the values that would be measured in three different two-component systems. The first system consists of 20% of the short component, the second 50%, and the third 80%. These three configurations demonstrate the ability of the algebraic method. As can be seen in Table II, there is some error involved in using this technique. The error, however, is less than the typical error of the fluorescence-lifetime imaging systems presented in this chapter. For an integration time of several seconds, an error of 0.4° in phase and 0.005 in modulation is normal. This magnitude of error results in about a 1% error in the lifetime at the appropriate frequency. If smaller errors are required, the algebraic method could be performed interatively, or the measured phase and modulation could be fitted to a two-component model using standard fitting routines.

C. Photobleaching Effects

Fluorescence photobleaching (photon-induced destruction of the fluorophore) is a major problem in fluorescence microscopy. This can make quantitatively reproducible intensity measurements next to impossible. Lifetime measurements, however, should be insensitive to such a loss of fluorophores. However, a problem can still arise if the concentration changes significantly during a lifetime measurement. In this section, lifetime-measurement errors caused by photobleaching are compared for three frequency-domain data acquisition methods.

Table I
Phase and Modulation Values of Three Two-Component Systems at Two Sample Frequencies

		ϕ_r (ω_1)	M_r (ω_1)	ϕ_r (ω_2)	M_r(ω_2)
20% short	80% long	32.5°	0.170	25.0°	0.853
50%	50%	32.2°	0.424	14.7°	0.888
80%	20%	32.1°	0.678	5.5°	0.948

Note. $\omega_1 = 2\pi\cdot 100$ MHz, $\omega_2 = 2\pi\cdot 100$ kHz.

Table II
Results of the Numerical Separation of Different Lifetime Components in the Three Sample Systems

	20% τ_1		50% τ_1		80% τ_1	
value	result	error	result	error	result	error
f	0.2016	0.8%	0.5011	0.2%	0.8004	0.05%
τ_1	1.014 ns	1%	1.002 ns	0.2%	0.998 ns	0.2%
τ_2	1.004 μs	0.4%	1.002 μs	0.2%	1.010 μs	1%

In the comparison, each method was given the same amount of time to observe the sample, and all methods collected four phase samples per integration cycle.

The first method investigated is heterodyning. The cross-correlation frequency was 32 Hz, and integration was performed by synchronous averaging. The second method is normal homodyning. The detector was modulated at the four phase angles 0°, 90°, 180°, and 270°. Each phase was integrated for one-quarter of the total integration time. The third method is modified homodyning. For this method, the detector was modulated at the same four phase angles, but the phase was first stepped up and then back to counteract trends caused by photobleaching. The phase steps and order were 0°, 90°, 180°, 270° and then 270°, 180°, 90°, and 0°. Each phase step was integrated one-eighth of the total time and intensities at corresponding phase angles were averaged.

To compare the three acquisition methods, two samples were produced: one that exhibited strong photobleaching and one that had insignificant photobleaching. For both samples, DAPI (4,6-diamidino-2-phenylindole; Sigma Chemical, St. Louis, MO), a common fluorescent probe, was chosen. This probe is quite easily photobleached. The nonphotobleaching sample was a solution of DAPI loaded into a hanging drop slide. The bleaching in this sample was negligible because of the diffusion of fresh DAPI molecules from outside the excitation volume. For the photobleaching sample, the effects of diffusion were limited by using a polyacrylimide gel commonly used for gel chromatography (Bio-Gel P6, exclusion limit 6 kD; Bio-Rad, Richmond, CA). When a sample volume of the gel was photobleached, no return of the fluorescence intensity to its original value was observed even after several minutes. The lifetime and photobleaching rate were constant in these samples.

Figure 4 shows a representative photobleaching decay in the photobleaching-sensitive system. The intensity decrease was fitted to a double exponential model that resulted in a short photobleaching time of 9 seconds and a long photobleaching time of 140 seconds. The double exponential fit suggests a dual rate process. The origin of the processes is not known. To avoid the effects of the fast component, all of the photobleaching samples were illuminated for at least 30 seconds before lifetime data was acquired.

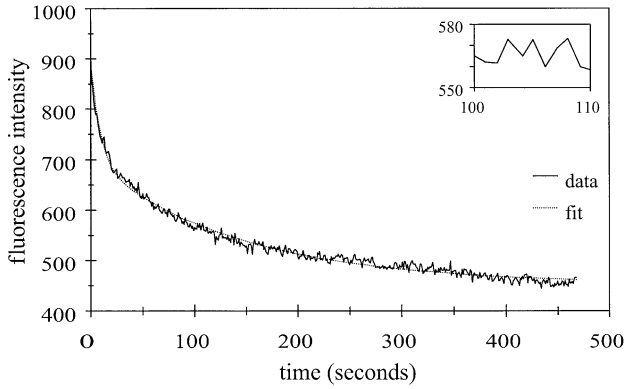

Fig. 4 Fluorescence intensity of DAPI as a function of time showing photobleaching. The bleaching effects were fit to a double exponential decay with decay times of 9 and 140 seconds.

Phase and modulation errors of the three data collection methods are shown in Fig. 5. For the bleaching measurements, the errors for the various integration times were calculated by comparing the longer integration measurements to the average of reference measurements. As a reference for each method, the phase and modulation were measured for 10 seconds repeatedly. During this short integration time, photobleaching caused little change in average intensity (as shown in the inset of Fig. 4). Consequently, photobleaching should have little effect on the phase and modulation during the reference measurements using any method. The errors presented are the average errors of four to eight different samples at each integration time. The graph clearly shows that the heterodyning acquisition method is the least affected by photobleaching. This is an important factor in our choice of the heterodyning acquisition method for fluorescence-lifetime imaging microscopy.

III. Fluorescence-Lifetime-Resolved Camera

The fluorescence-lifetime-resolved camera uses a CCD detector to collect nanosecond time-resolved data in parallel. The camera system can simultaneously measure fluorescence lifetime at every point in a microscopic image. It uses a high-speed CCD camera modified to collect lifetime data. The heterodyning technique coupled with a fast camera yields several unique advantages over previously reported camera systems (Lakowicz and Berndt, 1991; Wang *et al.*, 1991; Gadella *et al.*, 1993; Oida *et al.*, 1993; Morgan *et al.*, 1995; McLoskey *et al.*, 1996). First, this instrument is capable of generating lifetime images in a few seconds. Second, it minimizes the effect of photobleaching, a common problem in microscopy.

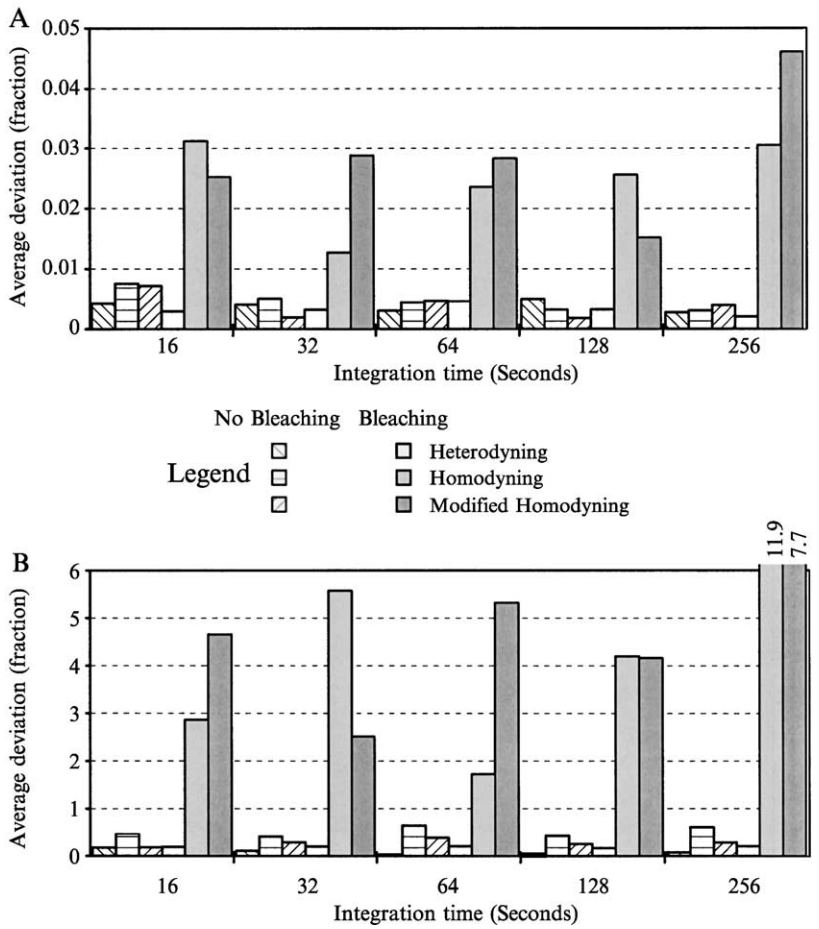

Fig. 5 Comparison of three data acquisition methods in the presence and absence of photobleaching. The average deviation is the average of the magnitude of the error of several measurements. (A) Modulation; (B) phase.

This system can operate in the presence of high background fluorescence and can quantitatively measure lifetimes of microscopic samples. Time-resolved imaging can not only effectively and selectively enhance the contrast of microscope fluorescence images but also quantitatively measure lifetimes within cellular compartments to monitor their microenvironment. With an acquisition rate as short as a few seconds, kinetic studies of lifetime changes are also possible with this camera.

A. Instrumentation

Our first camera system was constructed using a CCD camera coupled to an image intensifier (So *et al.*, 1994). Subsequently, a second-generation lifetime-resolved camera was constructed of a scientific-grade high-speed CCD and a custom image intensifier. The second-generation instrument addressed problems with the CCD, frame rate, modulation frequency, and other troubles. Throughout the development, the optics and data acquisition remained essentially the same. A general schematic of the instrument is illustrated in Fig. 6.

1. Camera and Image Intensifier

The two most important components of the lifetime-resolved camera system are the CCD and the microchannel plate image intensifier. The second-generation camera includes a scientific-grade CCD (CA-D1-256, Dalsa, Waterloo, Ontario). This CCD operates in the progressive-scan mode as opposed to the interlaced mode. Its frame rate is variable (derived from an external signal) and can be as high as 200 Hz. The new CCD also has a signal-to-noise ratio of 70 dB. The resolution is 256 × 256 pixels, each with an area of 16 × 16 μm^2. Although we could have chosen a camera with higher resolution, we chose one that has a lesser resolution but that can operate at a faster frame rate. The microchannel plate is coupled via fiber-optics to the CCD. It was custom built by Hamamatsu (model V6390U, Bridgewater, NJ) for high-speed modulation. It has a double-stage

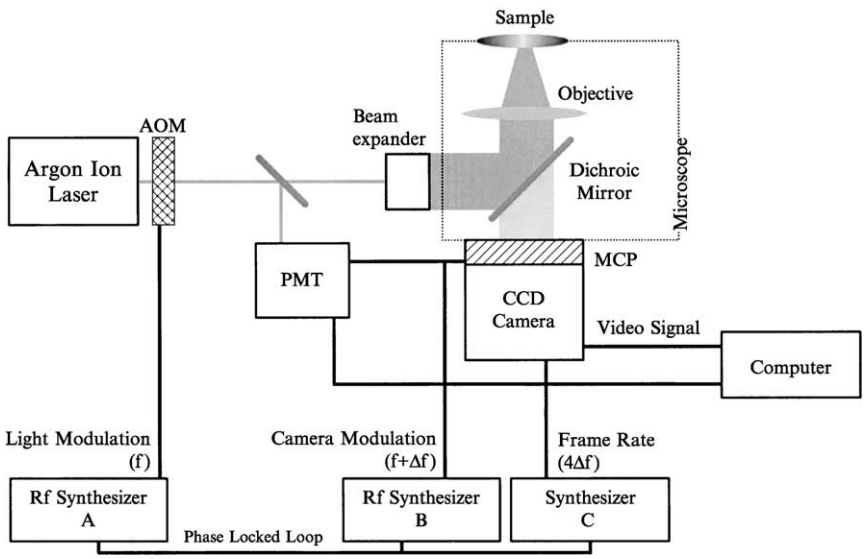

Fig. 6 Camera-based fluorescence-lifetime imaging microscope schematic.

design with a gain of approximately 10^5. The camera is gain modulated by modulating the cathode of the microchannel plate (So *et al.*, 1994). We have tested the modulation to 500 MHz.

2. Light Source and Optics

To illuminate the sample, a laser is directed into an epifluorescence microscope (Axiovert 35, Zeiss Inc., Thornwood, NY). The laser beam is coupled via fiber-optic to a beam expander and then delivered to the microscope for wide-field illumination. Shown in Fig. 6 is an argon ion laser (model 2025, Spectra Physics, Mountain View, CA) modulated by an acousto-optical modulator (AOM; Intra-Action, Belwood, IL). The argon ion laser can provide illumination at several selected blue-green wavelengths, most notably 514 and 488 nm. The acousto-optical modulator can optically modulate light at discrete frequencies from 30 to 120 MHz. One particular benefit of an AOM is its high throughput (up to 50%). As an alternative to the AOM, a Pockels cell (ISS Inc., Champaign, IL) was also used. The Pockels cell has the advantage of modulating at any frequency from 0 to 300 MHz. The advantage of continuous wide-band modulation is offset by the relatively poor throughput (~5%). Another alternative modulated light source used in our experiments was a cavity-dumped DCM dye laser (model 700, Coherent Inc., Palo Alto, CA) synchronously pumped by a Nd:YAG laser (Antares, Coherent Inc.). The dye laser produces 10-ps pulses at a range of frequencies. The frequency can be chosen by the cavity dumper to be any integer divisor (4–256) of the Nd:YAG fundamental frequency (76.2 MHz). The narrow pulse width insures that there will be harmonics measurable to many gigahertz. The dye laser provides a tunable source in the near UV region (300–340 nm).

3. Data Acquisition

The data acquisition scheme plays an important part in the performance of the camera system. The hardware determines the sensitivity and time response of the system, whereas the software provides a user interface and noise/artifact reduction. The camera has an 8-bit digital output. The output signal is sent to an Image-1280 digitizer (MATROX Electronic Systems Ltd., Dorval, Quebec). Four frames are collected per cross-correlation period. The cross-correlation frequency of the system is from 1–50 Hz. Each frame is synchronously averaged with the corresponding frame of the previous cross-correlation period. The Image-1280 can average the frames and transfer the averaged frames to the host computer without interrupting image acquisition. Hence there is no limit on the number of cross-correlation periods that can be averaged. After collecting the average cross-correlation images, the phase and modulation are independently calculated for each point in the image. Measurements of typical fluorescence probes generally result in an uncertainty of about 200 ps, which can be achieved in about 300 cross-correlation periods (30 seconds at 10 Hz).

Although the camera can record internally consistent phase and modulation images, there is no guarantee that the values in different images are comparable. In general, the high-frequency modulation signals change slightly between measurements. Slow phase and modulation drifts are common in acousto-optical and electro-optical modulators. To account for these small variations, a second detector is used to monitor the laser light source. All values calculated for an image are referenced to the monitor values. The detector that monitors the laser is a photo-multiplier tube (PMT; R928, Hamamatsu, Bridgewater, NJ), and data from the PMT are digitized with a second digitizer (A2D-160, DRA Laboratories, Sterling, VA).

B. Camera-Based Microscope Examples

Lifetime images of some simple microscopic systems were obtained to test the performance of this fluorescence-lifetime imaging microscope. The following examples demonstrate the ability of our microscope to selectively enhance image contrast and to quantitatively measure fluorescence lifetime.

One of the most important features of the lifetime microscope is its ability to measure minute differences in cellular microenvironments in which fluorescence-intensity measurements do not have sufficient sensitivity. As a demonstration, we imaged a string of live spirogyra cells (Fig. 7). Spirogyra cells organize as long strands, with cells connected end to end. The most prominent features in each of these cells are the large, double-helical chloroplasts. The chlorophyll in these organelles is brightly fluorescent when illuminated at 514 nm. The string of cells was imaged with the time-resolved microscope at a modulation frequency of 81 MHz.

This image was taken at the junction between two distinct spirogyra cells. The break in the helical structures corresponds to the separating cell walls between the two cells. The cell walls (which have been drawn for clarity) are not visible, as they are not fluorescent. Judging from the fluorescence-intensity picture alone, these two cells appear to be identical. However, a significant difference in chlorophyll lifetimes in these two cells can be observed in the phase-resolved picture (Fig. 7B). Note that the chloroplast within each individual cell has a uniform lifetime that is distinct from the other. This observation shows that the nonuniformity in the phase-resolved picture reflects the environment of the chloroplast in the cells and is not caused by experimental artifacts of the lifetime camera. In the phase-resolved picture, the cell at the upper-right-hand corner has a higher phase value (and is more demodulated), whereas the other cell has a lower phase value (and is better modulated). This is consistent with the hypothesis that the chlorophyll of the cell at the upper-right corner has a longer lifetime. Because the growth of these cells was not controlled, the cause of the lifetime difference is unknown. This example demonstrates the promise of the time-resolved microscopy technique in quantitatively monitoring cellular functions.

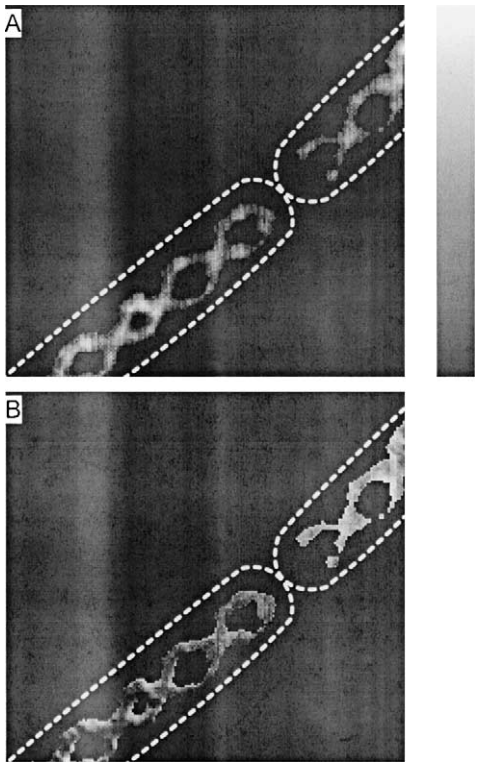

Fig. 7 Frequency domain pictures of chloroplast fluorescence of two spirogyra cells. (A) DC intensity (arbitrary units). (B) phase (0°–90°) at 81 MHz. The gray scale is linear from the minimum (black) to the maximum (white). The dotted line illustrates the cell walls.

As another demonstration of lifetime imaging, a two-layer fluorescent sample was imaged. In this sample, the well of a hanging drop slide was filled with a POPOP-ethanol solution and sealed with a coverslip. The second layer, placed on top of the fist, consisted of 15-μm blue fluorescent spheres (Molecular Probes, Inc., Eugene, OR) in water and was sealed with another coverslip. POPOP exhibits a single exponential decay in ethanol of 1.3 ns and served as an internal fluorescence lifetime reference. The two solutions were not allowed to mix together because different solvents were required for each probe. Frequency-domain pictures were taken at multiple frequencies from 8 to 140 MHz using the DCM dye laser. The phase differences and modulation ratios between the sphere and the dye background were measured at each frequency. Using the known lifetime of the POPOP background, the absolute phase shift and modulation of the sphere fluorescence were determined (Fig. 8).

The absolute phase shift and modulation values were analyzed using GLOBALS Unlimited (University of Illinois, Urbana, IL). As expected for a

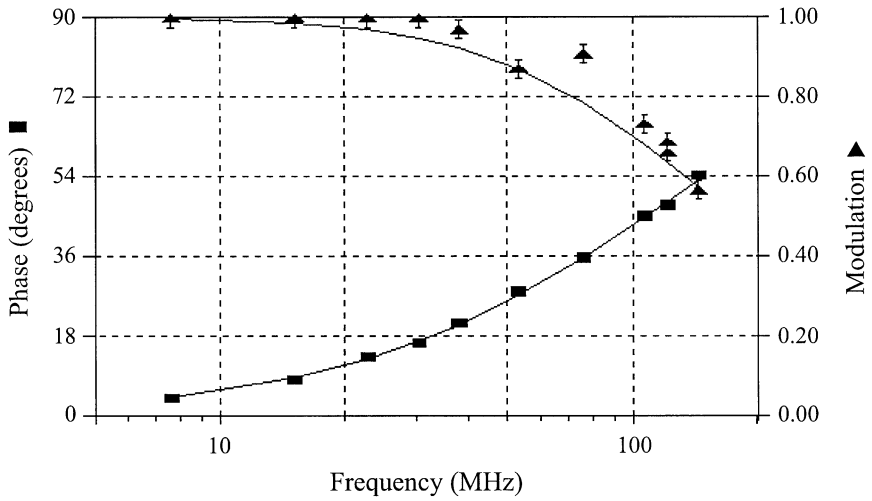

Fig. 8 Phase shift and demodulation of 15-μm fluospheres as a function of frequency. The data are the average value of all of the spheres in one image. The fit (solid line) is a double exponential fit. The phase error was 0.4° (error bars are smaller than the symbols), and the modulation error was 0.05.

two-species system, the data obtained fits best to a double exponential decay. One component was fixed to have the lifetime of POPOP, and the other was allowed to vary. From the intensity images, the POPOP was expected to contribute about 0.7 of the total intensity. The calculated fractions were 76% for POPOP and 24% (3%) for the sphere in close agreement with the intensity estimate. The lifetime of the spheres was calculated to be 2.5 ns (0.3 ns).

IV. Two-Photon Fluorescence Lifetime Microscopy

The second fluorescence-lifetime microscope design uses two-photon excitation and laser scanning to produce three-dimensional fluorescence-lifetime images. Two-photon excitation was first introduced to microscopy by Denk *et al.* (1990). In this technique, chromophores are excited by the simultaneous absorption of two photons, each having half the energy needed for the excitation transition (Friedrich, 1982; Birge, 1983; Birge, 1985). Because two photons are involved in the absorption process, the corresponding excitation probability is proportional to the square of the excitation power. The key for efficient two-photon excitation is a high temporal and spatial concentration of photons. Only in the region of a high photon density will there be appreciable two-photon excitation. The high spatial concentration of photons can be achieved by the diffraction-limited focusing of laser light using a high–numerical aperture objective. The high temporal concentration of photons is best accomplished using high-peak-power-mode-locked lasers.

Depth discrimination is the most important advantage of two-photon excitation microscopy. For one photon excitation in a spatially uniform fluorescent sample, equal fluorescence intensities are contributed from each z-section above and below the focal plane (assuming negligible excitation attenuation). This is a result of the conservation of energy (Wilson and Sheppard, 1984). In contrast, in two-photon excitation using objectives with a numerical aperture of 1.25, over 80% of the total fluorescence intensity comes from a 1-μm-thick region about the focal point (So *et al.*, 1995).

The spatial resolution and depth discrimination of the two-photon microscope are comparable to conventional confocal systems. For excitation of the same chromophore, the resolution is roughly half of that obtained under one-photon confocal microscopy (Sheppard and Gu, 1990). This reduction in spatial resolution is the result of the larger diffraction-limited spot achieved in focusing the longer-wavelength, two-photon excitation source (double the wavelength of the one-photon source). For our microscope, 960-nm excitation results in a FWHM (full width at half maximum) of the point-spread function 0.3 μm along the radial axis and 0.9 μm along the axial direction (So *et al.*, 1995).

Two-photon excitation also has the unique advantage that photobleaching and photodamage are localized to a submicron region at the focal point. In contrast, a conventional scanning confocal microscope causes photobleaching and photodamage anywhere within the illumination volume. In addition, no detection pinhole is required with a two-photon microscope to achieve axial depth discrimination. Because more fluorescence photons are required to generate high-quality time-resolved images than intensity imaging, the light-gathering efficiency is an important factor in the successful implementation of a time-resolved microscope. This requirement is critical in three-dimensional imaging in which the sample is exposed to a long period of laser excitation. Therefore, maximizing microscope detector efficiency and minimizing sample photobleaching are important design considerations.

Our instrument operates at a high cross-correlation frequency that provides lifetime information on a per pixel basis. The temporal resolution of this system is about 400 ps, which is slightly inferior to standard fluorometers, which have a resolution of about 25 ps. This result is expected given that the data acquisition time at each pixel is typically a million times shorter than the time used by a conventional fluorometer. Because of the heterogeneous nature of the cellular environment, it is seldom necessary to determine specimen lifetime to an accuracy comparable to the standard fluorometer.

A. Instrumentation

Presented in Fig. 9 is the schematic of the two-photon, time-resolved microscope. It consists of a laser scanning microscope and a high-peak-power laser. This system operates efficiently at the normal light levels of microscopy. It also can operate at very low light levels. The system can detect low-photon events

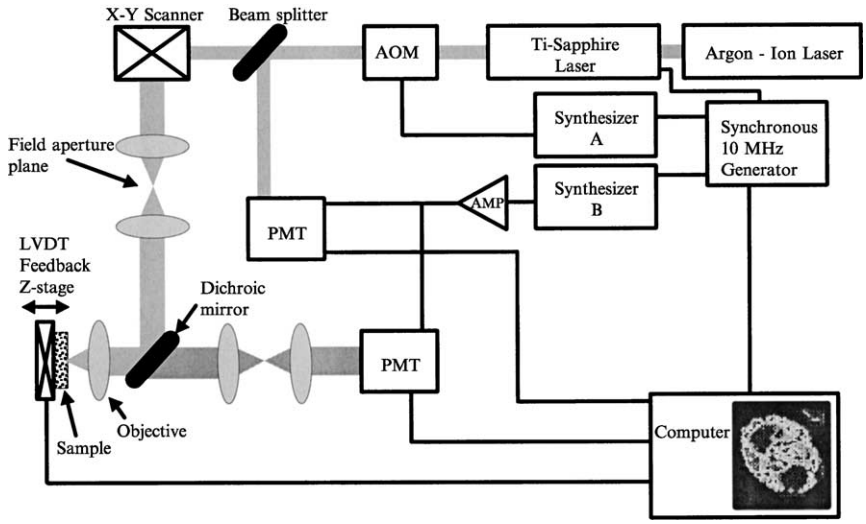

Fig. 9 Two-photon fluorescence-lifetime imaging microscope schematic.

(two to three photons) and has single-molecule detection capabilities. At the highest sensitivity, the background noise is equivalent to about one photon per pixel per frame.

1. Light Source

The laser used in this microscope was a mode-locked titanium sapphire (Ti-Sapphire) laser (Mira 900, Coherent Inc., Palo Alto, CA) pumped by an argon-ion laser (Innova 310, Coherent Inc., Palo Alto, CA). The features of this laser system are a high average power of up to 1 W, a high pulse repetition rate of 80 MHz, and a short pulse width of 150 fs. In addition, the intensity output of this laser is very stable, with typical fluctuations of less than 0.5%. Such stability is important for uniform excitation in the scanning system. The Ti-Sapphire laser has a tuning range from 720 to 1000 nm corresponding to one-photon excitation wavelengths of 360 to 500 nm. This wide tuning range allows most common near-ultraviolet, blue, and green fluorescent probes to be excited.

As a frequency-domain light source, the pulse train of the Ti-Sapphire laser has a modulation frequency content of 80 MHz and its harmonics. The harmonic content of the femtosecond pulse extends to terahertz. The lifetime determination of many common fluorescent probes requires the availability of modulation frequencies below 80 MHz. An acousto-optical modulator (Intra-Action, Belwood, IL) driven by the amplified signal of a phase-locked

synthesizer is used to generate these additional frequencies not available directly from the laser. This AOM has the desirable properties of low-pulse-width dispersion and high-intensity transmittance (typically 50%). Additional modulation frequencies can be generated by beating the AOM modulation with the 80-MHz laser pulse train and its harmonics. The mixing between the laser repetition frequency and the AOM modulation frequency generates new components at the sum and difference frequencies. This scheme allows one to generate intensity modulation from kilohertz to tens of terahertz (Piston *et al.*, 1989).

2. Optics and Scanner

An *x*-*y* scanner (Cambridge Technology, Watertown, MA) directs the laser light into the microscope. A low-cost single-board computer (New Micros, Inc., Dallas, TX) is the synchronization and interface circuit between the scanner and the master data acquisition computer. The master computer synchronizes the scan steps by delivering a TTL trigger pulse to the interface circuit, which outputs the required 16-bit number to move the scanner to the next pixel position. The normal region is a square of 256 × 256 scanned in a raster fashion. The scanner can scan over its full range with a maximum scan rate of 500 Hz. This rate limits the scan time needed for a typical 256 × 256-pixel region to be about 0.5 seconds, which corresponds to a pixel residence time of 8 μs. For normal operation, the pixel spacing in the images was 0.14 μm but could be adjusted as needed.

The excitation light enters the microscope (Axiovert 35, Zeiss Inc., Thronwood, NY) via a modified epiluminescence light path. The light is reflected by the dichroic mirror to the objective. The dichroic mirror is a custom-made short-pass filter (Chroma Technology Inc., Brattleboro, VT) that maximizes reflection in the infrared and transmission in the blue-green region of the spectrum. Because tight focusing increases the photon density, a high–numerical aperture objective is critical to obtain efficient two-photon excitation. The objective normally used is a well-corrected Zeiss 63× Plan-Neofluar lens with a numerical aperture of 1.25. The objective delivers the excitation light and collects the fluorescence signal. The fluorescence signal is transmitted through the dichoric mirror and refocused onto the detector. Because two-photon excitation has the advantage that the excitation and emission wavelengths are well separated (by 300–400 nm), suitable short-pass filters eliminate most of the residual scatter with a minimum attenuation of the fluorescence signal. In the excitation region of 900–1000 nm, we use 3 mm of BG39 Schott filter glass. It has an optical density of over 15 for the excitation wavelength while retaining over 80% of the transmittance in the fluorescence wavelength.

The *z*-axis position of the microscope stage is controlled by a second single-board computer (Iota System Inc., Incline Village, NV). The distance between the objective and the sample is monitored by a linear variable differential transformer (LVDT; Schaevitz Engineering, Camden, NJ). The LVDT output is digitized, and the single-board computer compares the measured position with the preset

position. The position of the objective is dynamically maintained by the computer, which drives a geared stepper motor coupled to the standard manual height-adjustment mechanism of the microscope. This control system is designed to have a position resolution of 0.1 μm over a total range of 200 μm. This dynamic feedback control system has a bandwidth of about 10 Hz.

3. Detector and Data Acquisition

A gain-modulated photomultiplier tube (model R3896, Hamamatsu, Bridgewater, NJ) detects the fluorescence signal from each position. A second gain-modulated photomultiplier tube (model R928, Hamamatsu, Bridgewater, NJ) monitors the laser beam to correct for frequency and modulation drift of the laser pulse train. The analog outputs of the two PMTs are digitized by the data acquisition computer.

One unique feature of this microscope is its high cross-correlation frequency. A high frequency ensures that complete cross-correlation waveforms can be collected within a minimum pixel residence time. A short pixel residence time is essential to achieve an acceptable frame refresh rate. The absolute minimum pixel residence time is limited by the mechanical response of the scanner to about 8 μs. However, the minimum residence time is actually limited by the digitizer and the number of photons available. The digitizer used in this instrument can operate at 60 kHz in simultaneous dual channel mode (12-bit resolution; A2D-160, DRA Laboratories, Sterling, VA). Data is acquired at four points per cross-correlation period. Thus, the digitizer limit is 70 μs per pixel (15 kHz). To make the timing easier, the actual maximum frequency is chosen to be 12.5 kHz (80 μs per pixel). At this rate an entire 256 $\times$ 256 frame can be acquired in just over 6 seconds. For fluorescence photon fluxes less than 10^7 per second, the pixel residence time should be increased to reduce statistical noise. As has been discussed, the most efficient way to reduce noise is to average over a few waveforms at each pixel. In this instrument, at least two waveforms are averaged, which brings the pixel residence time to 160 μs, which corresponds to a frame rate of about 13 seconds.

B. Two-Photon Microscopy Examples

The time resolution of this microscope was studied by imaging latex spheres labeled with chromophores of different lifetimes (Molecular Probes, Eugene, OR). Orange fluorescent latex spheres (2.3 μm in diameter) were mixed with Nile red fluorescent latex spheres (1.0 μm in diameter). The lifetime of these spheres was independently measured in a conventional cuvette lifetime fluorometer (ISS, Champaign, IL). The orange and red spheres each show a single exponential decay with a lifetime of 4.3 and 2.9 ns, respectively.

An image of two orange spheres (the larger ones) and three red spheres (the smaller ones) is presented in Fig. 10. Note that the small red sphere at the right edge of the picture has the same intensity as that of the larger orange spheres and

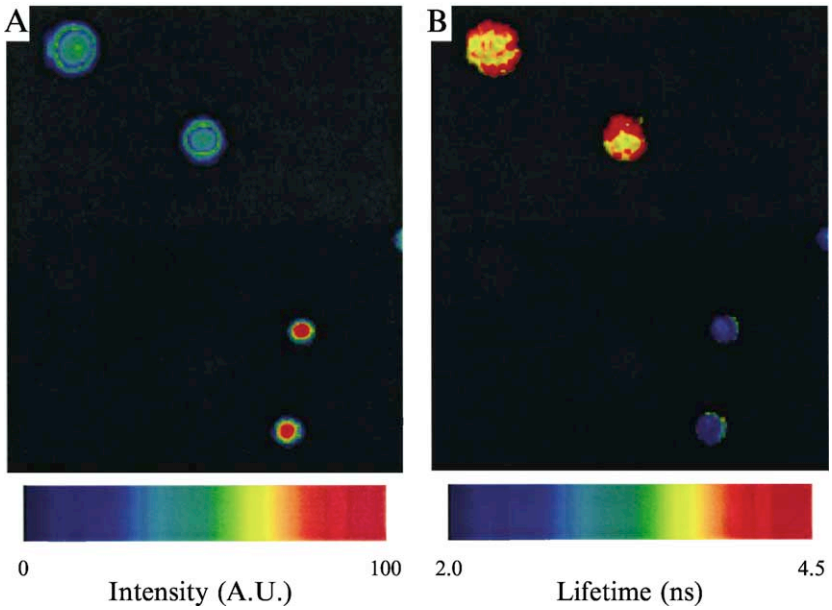

Fig. 10 Time-resolved image of orange (2.3 μm in diameter) and red (1.0 μm in diameter) fluorescent latex spheres. (A) Intensity; (B) lifetime.

is significantly less intense than the other red spheres. This observation stresses the fact that intensity is a poor parameter for discerning the property of the specimen in a fluorescence image. Intensity differences can be the result of differences in concentration and many experimental artifacts such as the uniformity of the illumination and detector response. In contrast, the lifetime picture shows lifetime values of 4.0 0.2 and 2.6 0.2 ns, in good agreement with the data obtained in the conventional fluorometer. The sphere on the right is correctly identified only in the lifetime picture.

Fluorescence-lifetime imaging is most valuable in cellular systems. As an example, FITC-dextran (FITC, fluorescein-5-isothiocyanate isomer I) was used to observe the pH in the vacuoles of mouse macrophages. The three-dimensional resolution of the two-photon microscope proved to be crucial in distinguishing closely packed vacuoles. Out-of-focus vacuoles contributed minimal fluorescence to the measured lifetime images.

Macrophages were incubated with 1 mg/mL FITC-dextran (Sigma Chemical; 50.7 kD, 1.2 mol FITC per mol dextran) for 24 hours before observation. The cells were not washed before examination. Fluorescence was observed only in vacuoles and in the extracellular media (Fig. 11). The average lifetime measured in the extracellular fluid was 3.9 ns, corresponding to a neutral pH, whereas the lifetime measured in the vacuoles was 3.1 ns on average, indicating an average intravacuolar

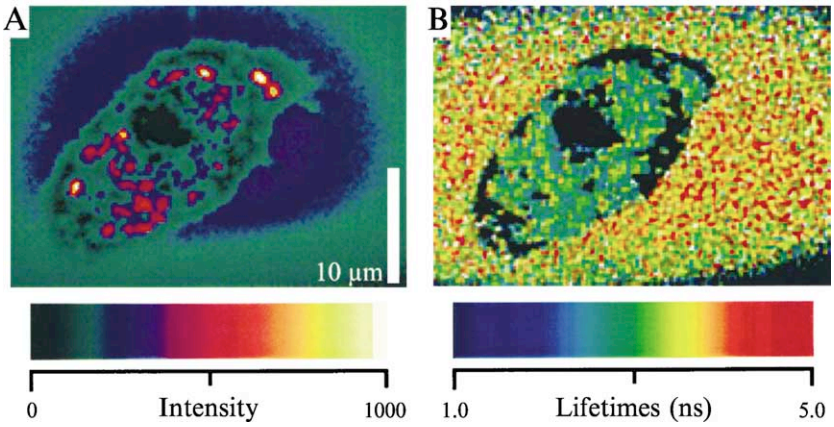

Fig. 11 Unwashed macrophages incubated 24 hours with FITC-dextran. Cells were provided by the laboratory of Dr. E. W. Voss, Department of Microbiology, University of Illinois.

pH of 4.0, consistent with previous reports (Ohkuma and Poole, 1978; Tycko and Maxfield, 1982; Murphy *et al.*, 1984; Straubinger *et al.*, 1990; Aubry *et al.*, 1993). All vacuoles have roughly the same lifetime, indicating that the vacuoles are at the same pH even though the intensity varied dramatically within individual cells.

V. Pump-Probe Microscopy

The third example of a fluorescence-lifetime imaging microscope uses an asynchronous pump-probe technique. We have adapted a frequency-domain, pump-probe technique (Elzinga *et al.*, 1987) for use in microscopy. Pump-probe spectroscopy uses a pump pulse of light to promote the sample to the excited state and a probe pulse to monitor the relaxation back to the ground state. The most common implementation is transient absorption (Fleming, 1986). Recently, applications using pump-probe spectroscopy with stimulated emission have also been reported (Lakowicz *et al.*, 1994b; Kusba *et al.*, 1994). With stimulated emission, one can either measure the stimulated emission directly or the resulting change in fluorescence emission intensity. In our microscope, we measure the modulation in fluorescence emission from chromophores excited by a pump laser source and stimulated to emit by a probe laser.

In microscopy, the asynchronous pump-probe technique offers spatial resolution equal to confocal microscopy and provides high-frequency response of a fluorescence system without a fast photodetector. The principle of this technique is illustrated in Fig. 12. Two pulsed laser beams overlap at the sample. Their wavelengths are chosen such that one beam (pump) is used to excite the molecules

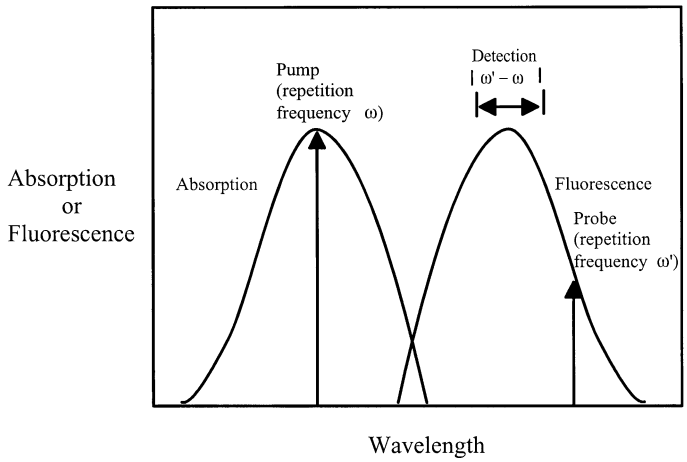

Fig. 12 Principles of the pump-probe (stimulated emission) technique.

under study and another beam (probe) is used to stimulate emission from the excited-state chromophores. The two laser pulse trains are offset in frequency by a small amount. This arrangement generates a fluorescence signal at the cross-correlation frequency and corresponding harmonics. Because the cross-correlation signal depends strongly on the efficient overlap of the two laser sources (Dong *et al.*, 1995; Dong *et al.*, 1997), superior spatial resolution and improved depth discrimination can be obtained by detecting the fluorescence at the beat frequency or its harmonics. Furthermore, pulsed laser systems can have high harmonic content. The low-frequency, cross-correlation signal harmonics correspond to the high-frequency laser harmonics. Therefore, a high-speed detector is not required to record the high-frequency components of the fluorescence signal.

A. Instrumentation

The experimental arrangement for our pump-probe fluorescence microscope is shown in Fig. 13. The design is quite similar to the two-photon microscope. The differences are mainly the result of the use of two laser beams instead of one. For example, the light sources are different, along with the excitation and emission filters. Also, the detector does not need to be gain modulated because the pump-probe signal is not at high frequency. Otherwise, the majority of the components are the same (such as the microscope, the *x*-*y* scanner, *z* (focus) positioner, and data acquisition software and hardware).

1. Light Sources

A master synthesizer that generates a 10-MHz reference signal is used to synchronize two mode-locked neodymium-YAG (Nd-YAG, Antares, Coherent

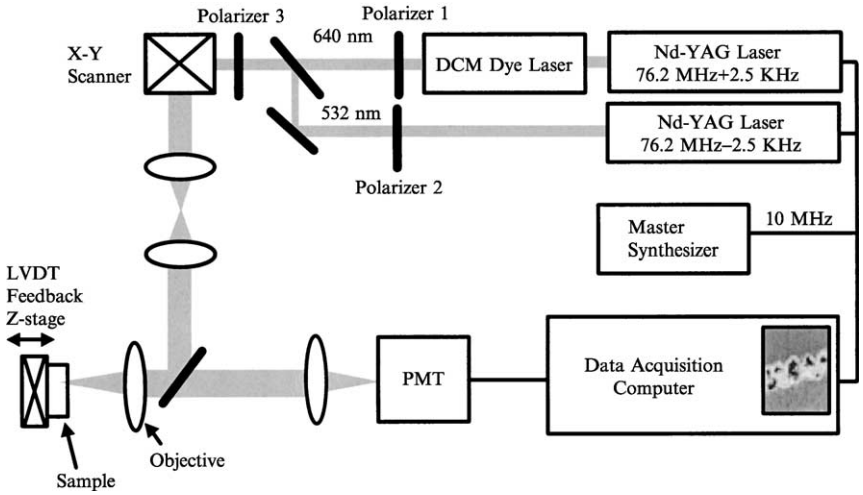

Fig. 13 Pump-probe fluorescence-lifetime imaging microscope schematic.

Inc., Santa Clara, CA) lasers and to generate a clock for the digitizer and scanner. The 532-nm output of the one Nd-YAG laser is used for excitation. The probe Nd-YAG laser pumps a DCM dye laser (Model 700, Coherent Inc., Santa Clara, CA) tuned to 640 nm and is used to induce stimulated emission. The pulse width (FWHM) of the pump laser is 150 ps, and the DCM probe laser has a pulse width of 10 ps. Combinations of polarizers are used to control the laser power reaching the sample. The average power of the pump and probe beams, at the sample, are about 10 μW and 7 mW, respectively. For time-resolved fluorescence microscopy, the pump source is operated at from 76.2 MHz to 2.5 kHz, and the probe laser's repetition frequency is 5 kHz away at 76.2 MHz + 2.5 kHz.

2. Optics

The two lasers are combined at a dichroic mirror (Chroma Technology Inc., Brattleboro, VT) before reaching the *x*-*y* scanner (Cambridge Technology, Watertown, MA). As with the two-photon system, the images are typically 256 × 256 pixels with a 0.14-μm pixel spacing. The beams are reflected into the microscope objective by a second dichroic mirror. To align the pump and probe lasers, we found it convenient to overlap their projections on the laboratory's ceiling.

Because tight focusing increases the photon density and localizes the pump-probe effect, a high–numerical aperture objective is used. The objective used in these studies is a well-corrected Zeiss 63× Plan-Neofluar with a numerical aperture of 1.25. With this objective, the optical point-spread function has a FWHM of 0.2 μm radially and 0.5 μm axially for excitation at 532 nm (Dong *et al.*,

1995). The fluorescence signal is collected by the same objective, transmitted through the second dichroic mirror and two 600 20-nm band-pass filters.

3. Detector and Data Acquisition

A PMT (model R928 or R1104, Hamamatsu, Bridgewater, NJ) detects the fluorescence signal from each position. The analog PMT signal is electronically filtered by a preamplifier (Stanford Research, Sunnyvale, CA) to isolate the 5-kHz, cross-correlation signal before being delivered to the data acquisition hardware and software. Typically we use a pixel dwell time of 800 μs, with a resulting frame acquisition time of 65 seconds.

4. Pump-Probe Polarization Microscopy and Laser Diode-Based Systems

There have been two technical developments in the pump-probe methodologies. First, it has been demonstrated that by varying the pump and probe orientation from the parallel/parallel to the parallel/perpendicular orientation, polarization microscopy can be achieved. As Fig. 14 shows, as the probe beam polarization samples the excited-state population, polarization measurements can be measured by rotating the probe beam orientation from parallel and perpendicular to the pump beam (Buehler *et al.*, 2000). This exciting development extends pump-probe microscopy to include polarization imaging capabilities. The second development in the pump-probe technique involves using intensity-modulated diode lasers as the pump and probe laser sources. Instead of using mode-locked pulse laser systems, economical intensity-modulated laser sources

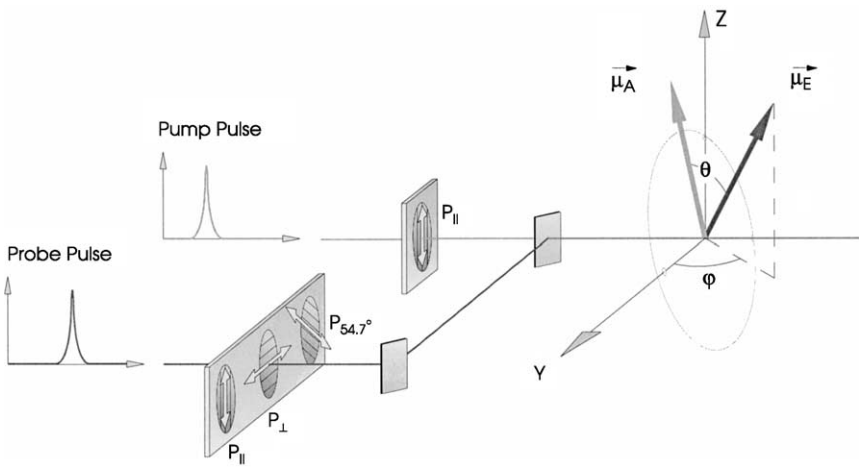

Fig. 14 Implementation of pump-probe polarization measurements. Polarization experiments can be performed by changing the relative orientations of the pump-probe beams from the ||/|| (parallel-parallel) to ||/⊥ (parallel-perpendicular) configurations.

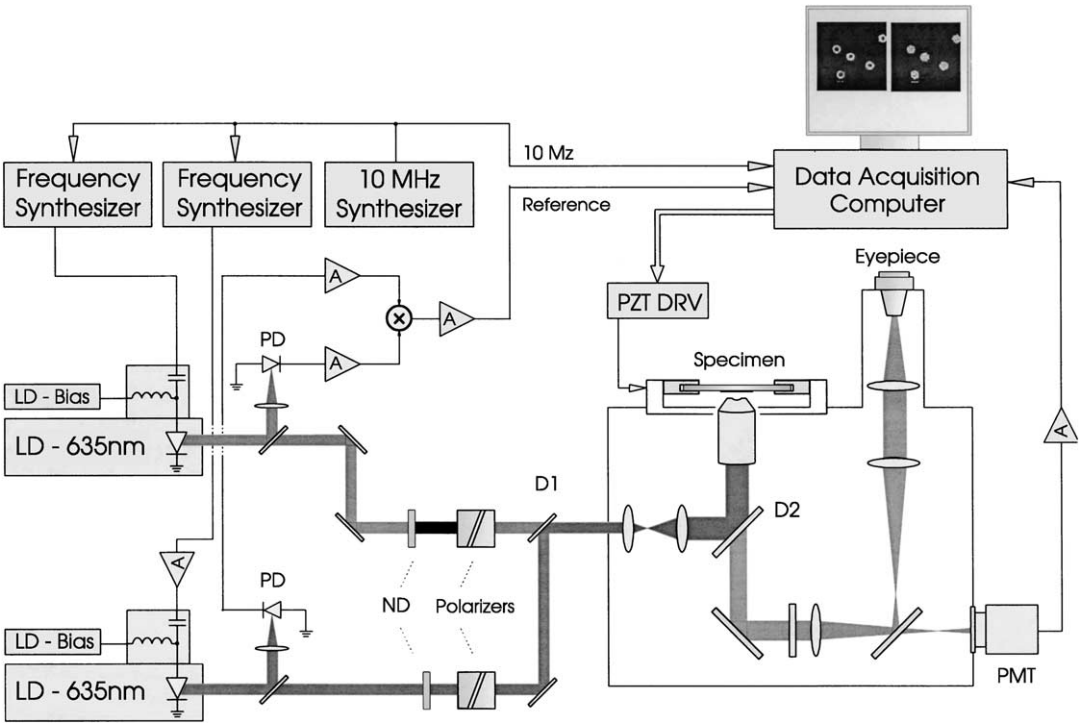

Fig. 15 Pump-probe fluorescence imaging using intensity-modulated laser diodes.

represent attractive alternatives and can contribute to popularizing the pump-probe methodology. A laser-diode-based pump-probe system is shown in Fig. 15. In this example, a sinusoidally modulated laser operating at 635 nm [Model APM 08(635-08), Power Technology Inc., Maybelvale, AR] is used as the excitation source. Another intensity-modulated laser diode at 680 nm [Model APM 08(690-40), Power Technology Inc., Maybelvale, AR] was used as the probe beam. The pump and probe beam modulation frequencies were 80 MHz and 80 MHz + 5 KHz, respectively (Dong *et al.*, 2001). For laser diodes operating in this range of wavelengths, the number of fluorescent species that can be used for pump-probe studies is rather limited. However, as the costs for the green and blue laser diodes drop, one can expect standard fluorescent molecules such as fluorescein or rhodamine to be used in laser diode–based pump-probe systems.

B. Pump-Probe Microscopy Examples

We obtained lifetime-resolved images of a mixture of 2.3 μm orange and 1.1 μm Nile-red (absorption maximum: 520 nm, emission maximum: 580 nm) fluorescent latex spheres (Molecular Probes, Eugene, OR). The two types of spheres were

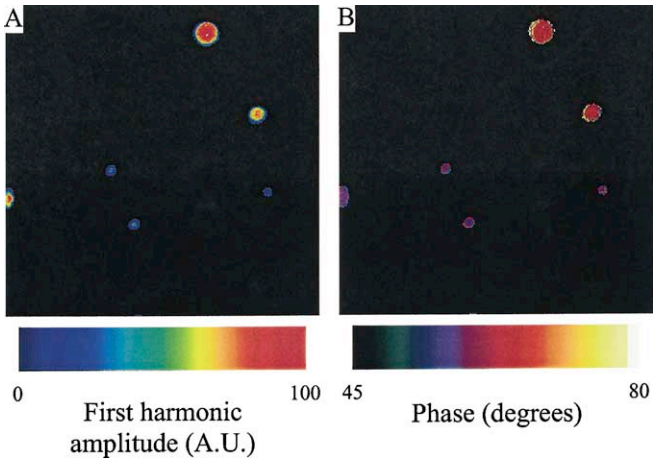

Fig. 16 Fluorescent lifetime images of 1.1-μm Nile-red (τ_p = 3.20 1.0 ns) and 2.3-μm orange (τ_p = 4.19 1.4 ns) fluorescent latex spheres. (A) First harmonic amplitude, (B) phase.

known to have different lifetimes. The measured lifetimes using a standard frequency-domain phase fluorometer are 2.70 ns for 1.1-μm spheres and 4.28 ns for 2.3-μm spheres. In our images, the first harmonic amplitude and phase are measured (Fig. 16). The phase image was referenced to that of a 4.16-mM rhodamine B slide for the purpose of lifetime calculations. From the histograms of lifetime values, the lifetimes of the spheres were determined to be 3.2 1.0 ns (1.1 μm) and 4.2 1.4 ns (2.3 μm). These values agree within error to the results from frequency-domain phase fluorometry.

We also examined mouse fibroblast cells doubly labeled with the nucleic acid stain ethidium bromide and the membrane stain rhodamine DHPE (Molecular Probes, Eugene, OR). The pump-probe image is shown in Fig. 17. These cells were grown on a coverslip and then fixed with acetone. The cells were stained first with ethidium bromide (1 mM in PBS, 0.1% Triton X-100) for 30 minutes and then stained by rhodamine DHPE (10 μg/ml in PBS, 0.1% Triton X-100) for another 30 minutes before it was rinsed twice in PBS and mounted for viewing. The lifetimes of the cytoplasmic and nuclear region were determined from the phase image. The reference phase was obtained from a slide of 4.16 mM rhodamine B in water. It was found that the average of lifetime histograms in the cytoplasm and nucleus are 2.0 0.5 s and 6.6 4.8 ns, respectively. For comparison, the lifetime of rhodamine B in water was determined in a standard frequency-domain phase fluorometer to be 1.44 ns. Furthermore, the lifetimes of the unbound ethidium bromide and bound ethidium bromide to nucleic acid are known to be 1.7 and 24 ns, respectively (So *et al.*, 1995). Our measurements of lifetime in cytoplasm show that there was significant staining of cytoplasmic structures by rhodamine DHPE. The average lifetime in the

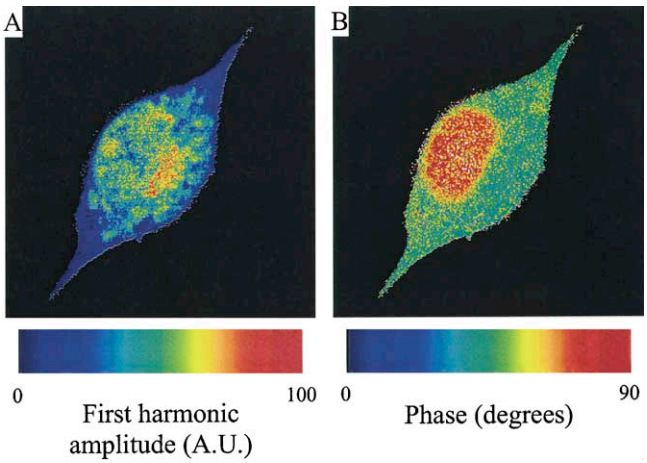

Fig. 17 Fluorescent-lifetime images of a mouse fibroblast cell labeled with rhodamine DHPE and ethidium bromide (membrane and cytoplasm: τ_p = 2.00 0.54 ns, nucleus: τ_p = 6.62 4.8 ns). (A) First harmonic amplitude; (B) phase. Cells were provided by the laboratory of Dr. M. Wheeler, Department of Animal Sciences, University of Illinois.

nucleus is between that of bound and unbound ethidium bromide, indicative of the fact that both populations of the chromophores exist in the nucleus. Nonetheless, the lifetime contribution from bound ethidium bromide is sufficient to distinguish the different lifetimes in the nucleus and cytoplasm as demonstrated by the phase image.

This example demonstrates one advantage of lifetime-resolved imaging. From intensity imaging, it is difficult to distinguish the cytoplasmic and nuclear regions, as these chromophores have similar emission spectra. With lifetime imaging, sharp contrast between the two species of chromophores can be generated.

As discussed, by rotating the pump and probe beam orientations, the pump-probe technique can also be used for polarization microscopy studies. Shown in Figs. 18 and 19 are examples of time-resolved, pump-probe images using this approach. In Fig. 18, the lifetime of a 15-μm orange fluorescent sphere (Molecular Probes, Eugene, OR) was determined to be 9.15 ns. In addition, one sees that the phase difference between the parallel/parallel (pump beam/probe beam) and parallel/perpendicular orientations is $\Delta\phi = \phi_{\|/\|} - \phi_{\|/\perp} = 5.8^\circ$. In this case, energy transfer most likely is the mechanism responsible for the depolarization. Another example of pump-probe polarization imaging is one in which a mouse fibroblast cell labeled with CellTracker CMTMR (Molecular Probes). As Fig. 19 shows, lifetimes of four different regions (I to IV) were determined to be 1.93, 2.75, 1.75, and 2.85 ns, respectively. As in the case of the 15-μm orange fluorescent sphere, by varying the relative pump and probe polarizations, the rotational correlation times for the four regions can also be determined. They are 27, 104, 107, and 151 ps for regions I to IV, respectively.

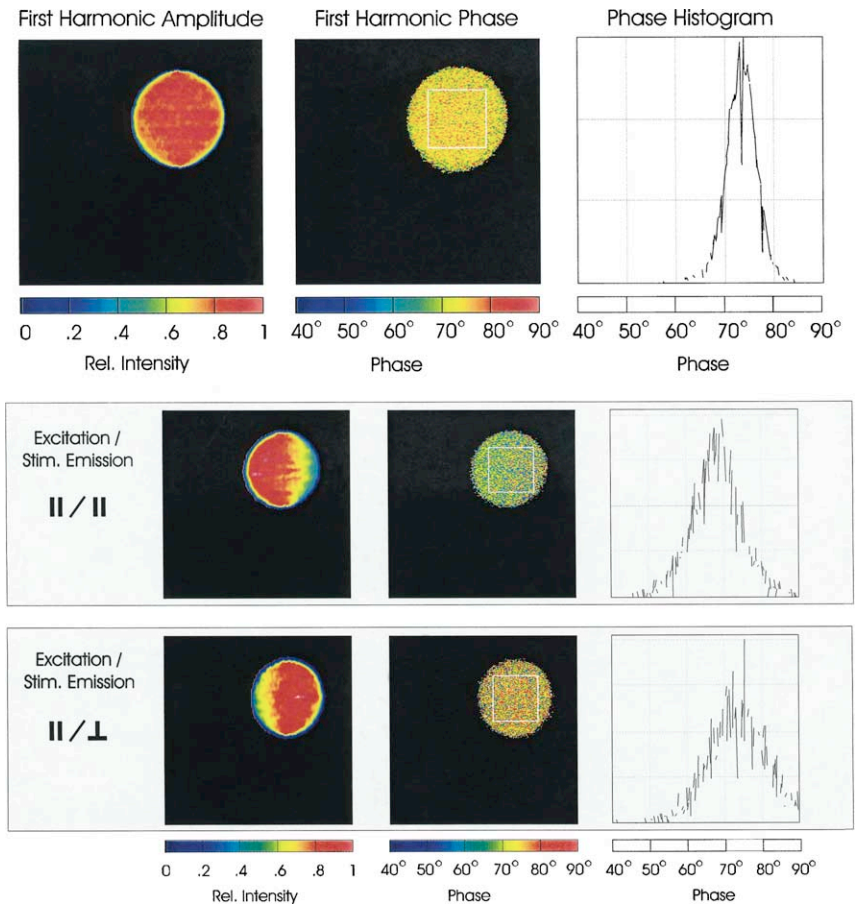

Fig. 18 Top: lifetime-resolved, first harmonic, pump-probe images of a 15-mm fluorescent latex sphere (lifetime 15 ns). Middle and bottom: lifetime-resolved, pump-probe polarization images of the same sphere in the $\|/\|$ and $\|/\perp$ configurations. $\Delta\phi = \phi_{\|/\|} - \phi_{\|/\perp} = 6^{\circ}$.

As the final example of pump-probe microscopy, an image of mouse STO cells labeled with TOTO-3 (Molecular Probes) is shown in Fig. 20. As the figure shows, the lifetime of the TOTO-3 labeled region is 1.81 ns. This example demonstrates that feasibility of using intensity-modulated laser diodes in pump-probe fluorescence imaging.

VI. Conclusion

Fluorescence-lifetime imaging provides the unique opportunity to study functional structures of living cellular systems. The three implementations of

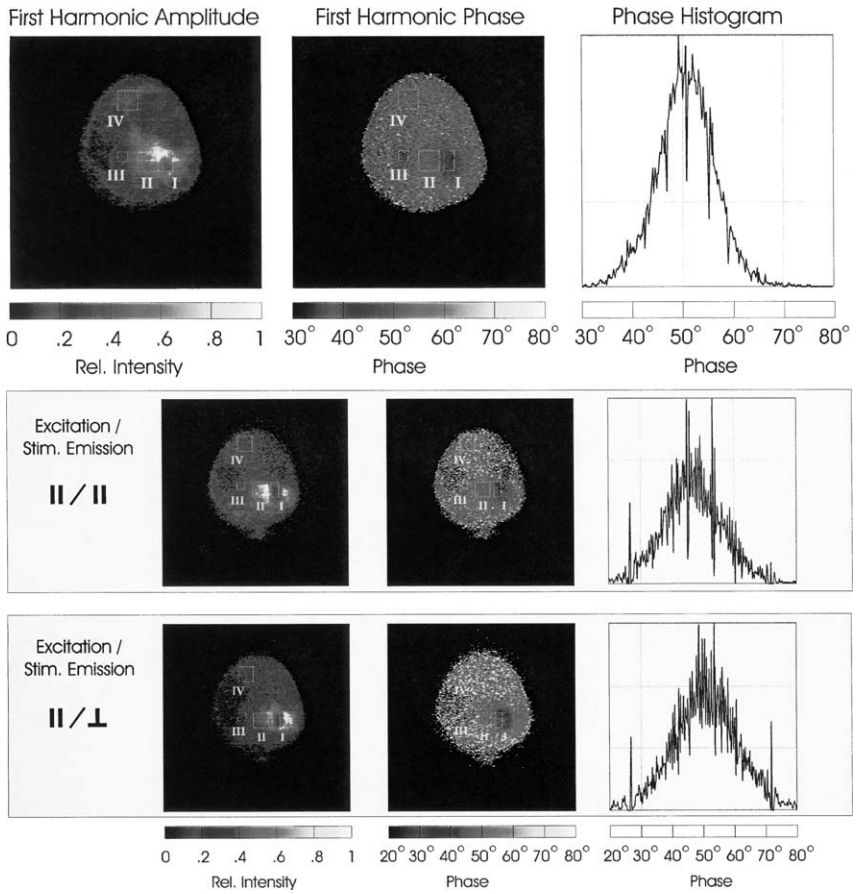

Fig. 19 Top: lifetime-resolved, pump-probe images of an orange CMTMR-labeled mouse fibroblast cell. Lifetimes in four regions were determined. In regions I to IV, the measured lifetimes were 1.93, 2.75, 1.75, and 2.85 ns, respectively. Bottom: lifetime-resolved, pump-probe polarization images of the same sphere in the ||/|| and ||/⊥ configurations. The rotational correlation times obtained from regions I to IV are 27, 104, 107, and 151 ps, respectively. The displayed histogram also demonstrates the global phase shift from the ||/|| to ||/⊥ orientations.

the lifetime-resolved microscope described in this chapter offer complimentary ways to solve similar problems. The lifetime camera captures all points in an image simultaneously, which is better for fast events and phosphorescence imaging. The laser scanning systems can image arbitrarily shaped regions of interest. Three-dimensional resolution is inherently part of both the two-photon and pump-probe implementations. The lifetime camera images, however, must be mathematically deconvolved to achieve three-dimensional resolution.

Each microscope presented has unique beneficial features. All three microscopes benefit from the frequency-domain heterodyning technique. The lifetime

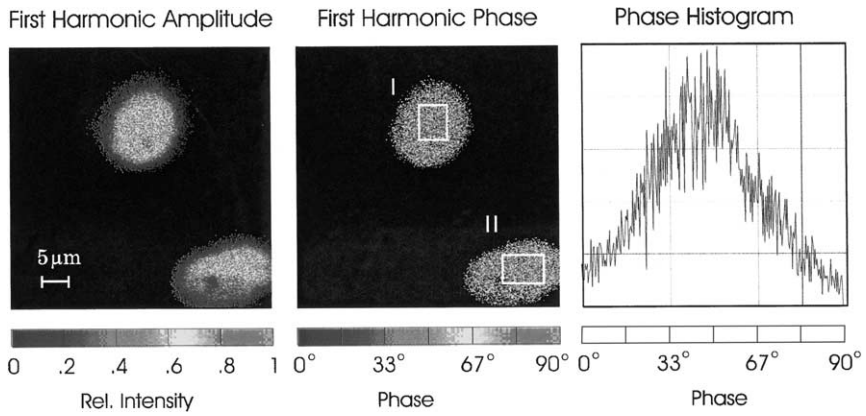

Fig. 20 Time-resolved, pump-probe image of mouse fibroblast cells labeled with TOTO-3. The average phase from regions I and II is 43°, corresponding to a fluorescence lifetime of 1.73 ns.

camera achieves high-speed imaging, high temporal resolution, and greater photobleaching resistance than existing camera alternatives. Compared with confocal detection, the two-photon microscope has better separation of excitation and emission light, better spatial confinement of photodamage, and similar resolution. The pump-probe microscope provides equal spatial resolution and effective off-focal background rejection while eliminating the need for high-speed detectors.

Fluorescence-lifetime imaging is a powerful technique that has far-ranging applications. Some projects that may be explored further are microscopic thermal imaging, multiple structure labeling of cells, and imaging and fluorescence in highly scattering media. Any process that needs nanosecond temporal resolution across an extended object is a good candidate. Fluorescence-lifetime imaging microscopy has the potential to dramatically enhance the field of fluorescence microscopy.

Acknowledgments

We thank Dr. Matt Wheeler, Dr. Laurie Rund, Ms. Linda Grum, and Ms. Melissa Izard in the Department of Animal Sciences, University of Illinois, for providing us with mouse fibroblast cells. We also thank Dr. Edward Voss, Dr. Jenny Carrero, Ms. Anu Cherukuri, and Mr. Donald Weaver in the Department of Microbiology, University of Illinois, for providing us with mouse macrophage cells. This work was supported by the National Institutes of Health grant RR03155.

References

Ambrose, W. P., Goodwin, P. M., Martin, J. C., and Keller, R. A. (1994). Alterations of single molecule fluorescence lifetimes in near-field optical microscopy. *Science* **265,** 364–367.

Aubry, L., Klein, G., Martiel, J.-L., and Satre, M. (1993). Kinetics of endosomal pH evolution in *Dictyostelium discoideum* amoebae. *J. Cell Sci.* **105,** 861–866.

Birge, R. R. (1985). Two-photon spectroscopy of protein-bound chromophores. *Acc. Chem. Res.* **19,** 138–146.

Birge, R. R. (1983). One-photon and two-photon excitation spectroscopy. *In* "Ultrasensitive Laser Spectroscopy" pp. 109–174. Academic Press, New York.

Buehler, C., Dong, C. Y., Dong, So, P. T. C., French, T., and Gratton, E. (2000). Time-resolved polarization imaging by pump-probe (stimulated emission) fluorescence microscopy. *Biophys. J.* **79,** 536–549.

Buurman, E. P., Sanders, R., Draaijer, A., Gerritsen, H. C., van Veen, J. J. F., Houpt, P. M., and Levine, Y. K. (1992). Fluorescence lifetime imaging using a confocal laser scanning microscope. *Scanning* **14,** 155–159.

Denk, W., Strickler, J. H., and Webb, W. W. (1990). Two-photon laser scanning fluorescence microscopy. *Science* **248,** 73–76.

Dix, J. A., and Verkman, A. S. (1990). Pyrene eximer mapping in cultured fibroblasts by ratio imaging and time-resolved microscopy. *Biochemstry* **29,** 1949–1953.

Dong, C. Y., Buehler, C., So, P. T. C., French, T., and Gratton, E. (2001). Implementation of intensity modulated laser diodes in time-resolved, pump-probe fluorescence microscopy. *Applied Optics* **40,** 1109–1115.

Dong, C. Y., So, P. T. C., Buehler, C., and Gratton, E. (1997). Spatial resolution in pump-probe microscopy. *Optik* **106,** 7–14.

Dong, C. Y., So, P. T. C., French, T., and Gratton, E. (1995). Fluorescence lifetime imaging by asynchronous pump-probe microscopy. *Biophys. J.* **69,** 2234–2242.

Elzinga, P. A., Kneisler, R. J., Lytle, F. E., King, G. B., and Laurendeau, N. M. (1987). Pump/probe method for fast analysis of visible spectral signatures utilizing asynchronous optical sampling. *Appl. Opt.* **26,** 4303–4309.

Feddersen, B. A., Piston, D. W., and Gratton, E. (1989). Digital parallel acquisition in frequency domain fluorimetry. *Rev. Sci. Instrum.* **60,** 2929–2936.

Fleming, G. R. (1986). "Chemical Applications of Ultrafast Spectroscopy" Oxford University Press, New York.

French, T., So, P. T. C., Weaver, Jr., D. J., Coelho-Sampaio, T., Gratton, E., Voss, Jr, E. W., and Carrero, J. (1997). Two-photon fluorescence lifetime imaging microscopy of macrophage mediated antigen processing. *J. Microsc.*

Friedrich, D. M. (1982). Two-photon molecular spectroscopy. *J. Chem. Education* **59,** 472–481.

Gadella, Jr, T. W. J., and Jovin, T. M. (1995). Oligomerization of epidermal growth factor receptors on A431 cells studied by time-resolved fluorescence imaging microscopy. A stereochemical model for tyrosine kinase receptor activation. *J. Cell Biol.* **129,** 1543–1548.

Gadella, Jr., T. W. J., Jovin, T. M., and Clegg, R. M. (1993). Fluorescence lifetime imaging microscopy (FLIM): spatial resolution of microstructures on the nanosecond time scale. *Biophys. Chem.* **48,** 221–239.

Keating, S. M., and Wensel, T. G. (1990). Nanosecond fluorescence microscopy: emission kinetics of Fura-2 in single cells. *Biophys. J.* **59,** 186–202.

König, K., So, P. T. C., Mantulin, W. W., Tromberg, B. J., and Gratton, E. (1996). Two-photon excited lifetime imaging of autofluorescence in cells during UVA and NIR photostress. *J. Microsc.* **183,** 197–204.

Kusba, J., Bogdanov, V., Gryczynski, I., and Lakowicz, J. R. (1994). Theory of light quenching: effects on fluorescence polarization, intensity, and anisotropy decays. *Biophys. J.* **67,** 2024–2040.

Lakowicz, J. R., Szmacinski, H., Lederer, W. J., Kirby, M. S., Johnson, M. L., and Nowaczyk, K. (1994a). Fluorescence lifetime imaging of intracellular calcium in COS cells using QUIN-2. *Cell Calcium* **15,** 7–27.

Lakowicz, J. R., Gryczynski, I., Bogdanov, V., and Kusba, J. (1994b). Light quenching and fluorescence depolarization of rhodamine B. *J. Phys. Chem.* **98,** 334–342.

Lakowicz, J. R., and Berndt, K. W. (1991). Lifetime-selective fluorescence imaging using an RF phase-sensitive camera. *Rev. Sci. Instrum.* **62,** 1727–1734.

Marriott, G., Clegg, R. M., Arndt-Jovin, D. J., and Jovin, T. M. (1991). Time resolved imaging microscopy. *Biophys. J.* **60,** 1374–1387.

McLoskey, D., Birch, D. J. S., Sanderson, A., Suhling, K., Welch, E., and Hicks, P. J. (1996). Multiplexed single-photon counting. 1. A time correlated fluorescence lifetime camera. *Rev. Sci. Instrum.* **67,** 2228–2237.

Morgan, C. G., Murray, J. G., and Mitchell, A. C. (1995). Photon correlation system for fluorescence lifetime measurements. *Rev. Sci. Instrum.* **66,** 3744–3749.

Morgan, C. G., Mitchell, A. C., and Murray, J. G. (1992). Prospects for confocal imaging based on nanosecond fluorescence decay time. *J. Microsc.* **165,** 49–60.

Müller, M., Ghauharali, R., Visscher, K., and Brakenhoff, G. (1995). Double pulse fluorescence lifetime imaging in confocal microscopy. *J. Microsc.* **177,** 171–179.

Murphy, R. F., Powers, S., and Cantor, C. R. (1984). Endosome pH measured in single cells by dual fluorescence flow cytometry: rapid acidification of insulin to pH 6. *J. Cell Biol.* **98,** 1757–1762.

Oida, T., Sako, Y., and Kusumi, A. (1993). Fluorescence lifetime imaging microscopy (flimscopy). *Biophys. J.* **64,** 676–685.

Ohkuma, S., and Poole, B. (1978). Fluorescence probe measurement of the intralysosomal pH in living cells and the perturbation of pH in various agents. *Proc. Natl. Acad. Sci. USA* **75,** 3327–3331.

Piston, D. W., Kirby, M. S., Cheng, H., Lederer, W. J., and Webb, W. W. (1994). Two photon excitation fluorescence imaging of three-dimensional calcium ion activity. *Appl. Optics* **33,** 662–669.

Piston, D. W., Sandison, D. R., and Webb, W. W. (1992). Time-resolved fluorescence imaging and background rejection by two-photon excitation in laser scanning microscopy. *Proc. SPIE* **1640,** 379–389.

Piston, D. W., Marriott, G., Radivoyevich, T., Clegg, R. M., Jovin, T. M., and Gratton, E. (1989). Wide-band acousto-optic light modulator for frequency domain fluorometry and phosphorimetry. *Rev. Sci. Instrum.* **60,** 2506–2600.

Sanders, R., Draaijer, A., Gerritsen, H. C., Houpt, P. M., and Levine, Y. K. (1995a). Quantitative pH imaging in cells using confocal fluorescence lifetime imaging microscopy. *Analytical Biochem.* **227,** 302–308.

Sanders, R., Draaijer, A., Gerritsen, H. C., and Levine, Y. K. (1995b). Selective imaging of multiple probes using fluorescence lifetime contrast. *Zoological Studies* **34,** 173–174.

Sheppard, C. J. R., and Gu, M. (1990). Image formation in two-photon fluorescence microscopy. *Optik* **86,** 104–106.

So, P. T. C., French, T., Yu, W. M., Berland, K. M., Dong, C. Y., and Gratton, E. (1995). Time-resolved fluorescence microscopy using two-photon excitation. *Bioimaging* **3,** 49–63.

So, P. T. C., French, T., and Gratton, E. (1994). A frequency domain time-resolved microscope using a fast-scan CCD camera. *Proc. SPIE* **2137,** 83–92.

Straubinger, R. M., Papahadjopoulos, D., and Hong, K. (1990). Endocytosis and intracellular fate of liposomes using pyranine as a probe. *Biochem* **29,** 4929–4939.

Tycko, B., and Maxfield, F. R. (1982). Rapid acidification of endocytic vesicles containing α_2-macroglobulin. *Cell* **28,** 643–651.

Wang, X. F., Uchida, T., Coleman, D. M., and Minami, S. (1991). A two-dimensional fluorescence lifetime imaging system using a gated image intensifier. *Appl. Spect.* **45,** 360–366.

Wang, X. F., Uchida, T., and Minami, S. (1989). A fluorescence lifetime distribution measurement system based on phase-resolved detection using an image dissector tube. *Appl. Spect.* **43,** 840–845.

Wilson, T., and Sheppard, C. (1984). "Theory and Practice of Scanning Optical Microscopy" Academic Press, New York.

Xie, X. S., and Dunn, R. C. (1994). Probing single molecule dynamics. *Science* **265,** 361–364.